A Confidence Measure for Assessing Optical Flow Accuracy in the Absence of Ground Truth

Patricia Márquez pmarquez@cvc.uab.cat
Debora Gil debora@cvc.uab.cat
Aura Hernàndez-Sabaté aura@cvc.uab.cat
Computer Vision Center, Campus UAB, Bellaterra, Barcelona

Abstract

Optical flow is a valuable tool for motion analysis in autonomous navigation systems. A reliable application requires determining the accuracy of the computed optical flow. This is a main challenge given the absence of ground truth in real world sequences. This paper introduces a measure of optical flow accuracy for Lucas-Kanade based flows in terms of the numerical stability of the data-term. We call this measure optical flow condition number. A statistical analysis over ground-truth data show a good statistical correlation between the condition number and optical flow error. Experiments on driving sequences illustrate its potential for autonomous navigation systems.

1. Introduction

Analysis of sequence motion arises in computer vision fields such as car driver assistance or autonomous navigation. To explore the properties of motion across image pixels, the computation of a dense flow field is mandatory.

Variational schemes are widespread powerful tools for computing dense motion vectors. They compute motion by finding the minimum of an energy functional [11] which combines two terms: the data-term and the smoothness-term. The data-term puts into correspondence one frame with the following one. Existing approaches use either the square of the original Optical Flow (OF) equation [11, 16, 20] or a metric associated to the system of equations provided by local techniques [8, 10, 6]. The smoothness-term determines the global properties of the vector field across the image.

There has been an increasing interest in developing variational schemes for minimizing over-regularization and keeping motion discontinuities [16, 17, 25, 20, 23, 26]. It follows that modern techniques are suitable for detection of unpredicted agents and occlusions in autonomous navigation applications. However their application to decision making in autonomous navigation systems might require discarding those regions where OF is neither reliable nor accurate. The most common way of measuring OF accuracy is by computing its deviation from the true motion vector. This suffices to quantify the overall performance, but it is useless at locating areas of poor performance in real-time application where no ground-truth is given.

The impact of poor performance is higher in local methods since they lack of a global regularizer. Thus, in early times, some local methods defined confidence measures in order to discard pixels where there is not enough information for a reliable estimate [5, 21, 22, 19]. But for [21], which uses the condition number [9], all of them base on the determinant of the matrix of the system involved in the computation of OF. Given that current variational schemes are more stable under a local drop of the data-term performance, the use of confidence measures has almost vanished. However, in dense flow fields we still need a confidence measure to determine in which points the estimation is reliable or not in the absence of ground truth. Since the energy functional follows from adding the local integrand for all pixels, in [8] they propose its evaluation at the computed flow field for assessing local reliability. As far as we know, this is the only confidence measure for variational approaches.

A main concern for detecting non-reliable regions in real-world sequences is that none of the above have correlated confidence measures with OF error. There are two main sources of error: a deficient design of the algorithm (ill-conditioned) and round-off numerical propagation errors. The former can not be predicted from OF equations and requires a thorough analysis of the algorithm properties. The latter can be analyzed using numerical stability concepts [9].

In spite of its simplicity, Lucas-Kanade [14] achieves successful results in a large range of applications such as car driving assistance or navigation systems [7, 18, 24]. In this paper we explore the main sources of error for frameworks having a data-term based on Lucas-Kanade equations. We also introduce a (local) confidence measure for such frame-

2011 IEEE International Conference on Computer Vision Workshops
978-1-4673-0063-6/11/$26.00

works (variational [8] or not [14]). Our confidence measure assesses points with unbounded error by encapsulating the conditions that ensure numerical accuracy of the data-term. We also present a validation protocol (including the design of synthetic data-bases and a statistical framework) for checking the statistical correlation between the confidence measure and the accuracy of the solutions to the local systems. Experiments on our synthetic sequences and the Middlebury database [2] show a good correlation between errors and our confidence measure. Its benefits for predicting the local reliability in autonomous navigation applications are illustrated on a driving assistance database [1].

The remains of the paper are organized as follows. In Section 2 we describe our error analysis for Lukas-Kanade schemes and present our confidence measure. Section 3 describes the experimental settings and section 4 the used databases. In Section 5 we show the results of the experiments and an application of the confidence measure to driving assistance sequences. Finally, in Section 6 there are the conclusions and future work.

2. Error analysis of Lucas-Kanade based schemes

The Lucas-Kanade (LK) approach [14] is based on the assumption that OF keeps constant in a neighborhood of each pixel of size σ. Under this assumption the approximation of the OF is computed minimizing the following function:

$$E_{LK}(w) = E_{LK}(u,v) = K_\sigma * \left((I_x u + I_y v + I_t)^2\right) \quad (1)$$

where $w = (u, v)$ denotes the optical flow, I an image sequence, subscripts denote partial derivatives (x and y denote spatial derivatives and t temporal ones), $*$ the convolution operator and K_σ a Gaussian kernel of standard deviation σ. The minimum satisfies $\partial_u E_{LK} = 0$ and $\partial_v E_{LK} = 0$, which gives the following system of equations:

$$\underbrace{\begin{pmatrix} K_\sigma * (I_x^2) & K_\sigma * (I_x I_y) \\ K_\sigma * (I_x I_y) & K_\sigma * (I_y^2) \end{pmatrix}}_{A_{LK}} \begin{pmatrix} u \\ v \end{pmatrix} = \underbrace{\begin{pmatrix} -K_\sigma * (I_x I_t) \\ -K_\sigma * (I_y I_t) \end{pmatrix}}_{b_{LK}} \quad (2)$$

Notice that A_{LK} is a symmetric matrix.

The LK approach can be formulated in global terms [8] using the following variational framework:

$$E_{LKV}(u,v) = \int E_{LK} + \alpha(|\nabla w|^2)\,\mathrm{d}x\,\mathrm{d}y \quad (3)$$

In order to avoid over-regularization in the flow field, the following non-quadratic functional can be used:

$$E_{LKV}(u,v) = \int \psi_1(E_{LK}) + \alpha\psi_2(|\nabla w|^2)\,\mathrm{d}x\,\mathrm{d}y \quad (4)$$

for $\psi_i(s^2) = 2\beta_i^2\sqrt{1+\frac{s^2}{\beta_i^2}}$, where β_i is a scaling parameter. The minimum of the functional is computed by means of the Euler-Lagrange system of equations:

$$\begin{aligned} \frac{1}{\alpha}\psi_1'(E_{LK})K_\sigma*(I_x^2u + I_xI_yv + I_xI_t) = \\ \mathrm{div}(\psi_2'(|\nabla w|^2)\nabla u) \\ \frac{1}{\alpha}\psi_1'(E_{LK})K_\sigma*(I_xI_yu + I_y^2v + I_yI_t) = \\ \mathrm{div}(\psi_2'(|\nabla w|^2)\nabla v) \end{aligned} \quad (5)$$

where $\psi_i'(s^2) = \frac{1}{\sqrt{1+\frac{s^2}{\beta_i^2}}}$ for $i = 1, 2$. Notice that for large values of β_i, $\psi_i'(s^2) \approx 1$ and we recover the quadratic approach. If we write (5) in matrix form:

$$\frac{1}{\alpha}\psi_1'(E_{LK})\left[A_{LK}\begin{pmatrix} u \\ v \end{pmatrix} - b_{LK}\right] = \begin{pmatrix} \mathrm{div}\left(\psi_2'(|\nabla w|^2)\nabla u\right) \\ \mathrm{div}\left(\psi_2'(|\nabla w|^2)\nabla v\right) \end{pmatrix} \quad (6)$$

we recover LK local formulation given by (2).

Given that LK approaches solve the linear system given by (2), we will determine their sources of errors by studying the properties and numerical stability of the system.

2.1. Design Errors

An algorithm is accurate in the measure that it properly models what has to be solved. Otherwise, its solution (even if it has not numerical errors) differs from the problem solution. In the case of LK there are two main aspects that might distort its description of motion.

On the one hand, LK technique is based on the assumption that OF keeps constant in a neighborhood of each pixel. For that, at those locations where there is a collision of different motions, LK can not properly model OF.

On the other hand, the matrix A_{LK} is the structure tensor or second moment matrix [12] and it describes the image local geometry by means of its eigenvalue decomposition. At points with a (unique) well defined orientation, the matrix might be singular (i.e. it is not invertible), so that, the system is undetermined. This might be the case at straight image contours, specially at horizontal and vertical image edges and flat regions. In contrast, at points with two or more different orientations, the system of equations has a unique solution. The typical case is at corners and junctions. Therefore, LK approach, can not solve properly the aperture problem neither in edges nor in flat regions.

2.2. Error propagation

Errors in the output data that come from errors in the input of the algorithm are called propagation errors. In our case, the error given by the input data is produced by the acquisition of the sequences.

The condition number [9] associated to a system of equations $Ax = b$, gives an upper bound of the error of the solution in relation with the error given in b. Given a square matrix A, if e is the error in b, then the error in the solution $x = A^{-1}b$ is $A^{-1}e$. The relative error in the solution to the relative error in b is the mentioned condition number and determines the error propagation. It is defined as follows:

$$\mathrm{K}(A) = \frac{\|A^{-1}e\|/\|A^{-1}b\|}{\|e\|/\|b\|} = \|A\|\|A^{-1}\| \tag{7}$$

for $\|\cdot\|$ a matrix norm. If we consider the L^2 norm and the matrix A is symmetric, the condition number simplifies to:

$$\mathrm{K}(A) = \frac{\lambda_{max}}{\lambda_{min}} \tag{8}$$

where λ_{max} and λ_{min} are the maximum and minimum eigenvalues of A, respectively.

The condition number range is $[1, \infty)$. For large values the propagation of input errors is bad (ill-conditioned problem), whereas for low values (near to one) errors in the output compare to input errors and the problem is well-conditioned. In other words, if the condition number is large, then, the output error is not bounded and it can take any value (errors comparable with the input data errors or higher errors in the output data). Meanwhile, if the condition number is close to one, the error of the output data is comparable with the error of the input data, and thus, the output data is reliable.

Since the condition number is not bounded, we propose the following equivalent measure:

$$\kappa(A) = \left(\frac{\lambda_{min}}{\lambda_{max}}\right)^2 \tag{9}$$

Notice that now, the range is $(0, 1]$. And thus, for small values the error propagation might be large, whereas for values near to 1 the error propagation will be small. We note that with this formulation, singularity of the system (2) cancels κ, so that, one of the design errors of LK is also under control. In order to avoid indetermination values due to a $0/0$ division, formula (9) is computed setting to zero such cases.

Since the LK matrix is symmetric, we propose $\kappa(A_{LK})$ given by (9) as a confidence measure that correlates with the accuracy.

3. Experimental settings

We present a novel statistical analysis to assess the correlation between the confidence measure and the optical flow accuracy. We also compare our confidence measure against the confidence measure proposed by [8]. For that, the following experiments have been performed:

- **Error prediction capabilities for local LK:** The goal of this experiment is to validate that the confidence measure is correlated with the accuracy of LK approach.
- **Error prediction capabilities for variational LK:** The goal of this experiment is to validate that after embedding LK into a variational framework confidence measures still correlate with accuracy.
- **Application to autonomous navigation:** We also present an application to driving assistance showing the computed OF and the confidence measure.

The gaussian kernel used for either local LK and variational LK is the following:

$$K_\sigma = \frac{1}{25}\begin{pmatrix} 1 & 3 & 1 \\ 3 & 9 & 3 \\ 1 & 3 & 1 \end{pmatrix} \tag{10}$$

For the variational LK we have used the implementation developed by [13] which is available at [3]. This implementation defines $\psi_i(s^2) = \sqrt{\beta_i^2 + s^2}$. Note that for this ψ_i we have a non-quadratic variational LK. The parameters are set to $\alpha = 0.02$ and $\beta_i = 0.001$.

In order to measure the accuracy between the ground-truth and the computed OF we have computed the End-Point Error (EE), defined as follows [4]:

$$EE = \|w_C - w_{GT}\|_2 \tag{11}$$

where w_C is the computed OF and w_{GT} is the ground-truth of the OF.

The confidence measure κ is correlated with EE if they have a decreasing dependency. Such dependency is statistically explored by means of the correlation between EE and κ, considered as random variables. Since the correlation might be non linear, we consider the Spearman correlation coefficient, ρ [15]. The Spearman correlation coefficient takes values in $[-1, 1]$, indicating a maximum positive correlation for value 1, and a maximum negative one for value -1. In order to check if the dependency is significant we have used a unilateral hypothesis test [15]:

$$TP1 : \begin{cases} H_0 : \rho \geq 0 \\ H_1 : \rho < 0 \end{cases} \tag{12}$$

Rejecting the null hypothesis, ensures, statistically, a decreasing dependency.

We have also explored the correlation of the confidence measure reported in [8] given by point-wise evaluation of the integrand of E_{LKV} at the solution. In this case, (E_{LKV}) is correlated with the EE if they have an increasing dependency. And it is because for small values of E_{LVK} we have properly minimized the functional and thus the error might

be small. For that, the Spearman correlation coefficient is computed by means of the following unilateral hypothesis test:

$$TP2: \begin{cases} H_0: \rho \leq 0 \\ H_1: \rho > 0 \end{cases} \quad (13)$$

Rejecting the null hypothesis, ensures, statistically, an increasing dependency.

4. Databases

In order to carry out our experiments the following databases have been used.

4.1. Synthetic Database

In order to analyze the relation between the proposed confidence measure and the accuracy of LK we need a sequence with ground truth and high resolution. In the fashion of [5], we have created a new synthetic database. This database has a displacement of one pixel and it contains three textured images (with different geometric shapes) with a moving object. We consider three types of motion:

- **Homogenous Motion(H):** The same motion for the whole image.
- **Single Motion (M):** The geometric shape moves over an static background.
- **Double Motion (D):** The geometric shape and the background move in different directions.

For each sequence we have considered eight different movements ($(cos\theta, sin\theta)$, $\theta = 0^o, 45^o, ..., 270^o, 315^o$), in combinations of two elements for double motion sequences.

Notice that with this database we ensure optimal conditions for local LK and, for variational LK we suppress any errors due to temporal warping schemes. Also notice that this is the base-line best performance.

4.2. Middlebury Database

In order to see if we still having the same relation with the error and the confidence measure in the variational framework and using warping techniques we use the Middlebury database [2], which contains real-life and synthetic sequences with ground-truth. Those sequences can contain displacements up to 20 pixels per frame. The sequences contain several independently moving objects, thin structures, shadows and foreground-background transitions.

4.3. Endepa Database

In order to apply the confidence measure into real-life sequences, we use the Endepa project database [1]. This database contains real-world car sequences with no ground truth. The images are taken from a moving car. Therefore, at the outskirts of the image the temporal resolution is low, while at the center of the image the resolution is rather high.

Synthetic Database

(a) Seq1 (b) Seq2 (c) Seq3

Middlebury Database

(d) Grove2 (e) RubberWhale (f) Urban2

Endepa Database

(g) ConstructionSite (h) CrazyTurn (i) InternOnBike

Figure 1: Representative samples of each database.

Figure 1 shows representative samples of each database: synthetic in first row, Middlebury in central row and Endepa in the last row.

5. Results

5.1. Error prediction capabilities for local LK

By the temporal resolution of Middlebury and Endepa databases (too low for a standard non-pyramidal LK scheme), this experiment can only be performed in our synthetic database.

In figure 2 we plot the confidence measure κ versus the end-point-error EE for local LK for 3 representative synthetic sequences: homogeneous motion for sequence 1 in fig. 2(a), single motion for sequence 2 in fig. 2(b) and double motion for sequence 3 in fig. 2(c). For each plot, point clouds show values for each type of sequence considering all movements. Since we expect a decreasing dependency between κ and EE, the plots should draw an hyperbola. That is, we expect high values of EE for values of κ close to 0, while low values of EE for values of κ close to 1. For all cases, we observe a clear decreasing dependency between κ and EE.

	H		M		D	
	κ		κ		κ	
	ρ	$p-$val	ρ	$p-$val	ρ	$p-$val
Seq1	-0.56	0.00	-0.62	0.00	-0.59	0.00
Seq2	-0.57	0.00	-0.64	0.00	-0.63	0.00
Seq3	-0.64	0.00	-0.58	0.00	-0.63	0.00

Table 1: Spearman test $TP1$ for local LK considering the Synthetic database.

Table 1 shows the Spearman coefficient ρ and the $p-$value for the unilateral test $TP1$. As expected, the Spearman correlation coefficient achieves negative values and $p-$values are at working precision 10^{-88}. These $p-$values show that the decreasing dependency is statistically significant. Still, since ρ is not -1, there are some points where the error is independent to the properties of LK definition. Such errors might be caused due to inherent errors in the sequence design. Since the synthetic sequences are created interpolating one frame with a specific motion, the motion of the sequence in some points might not be exact.

5.2. Error prediction capabilities for variational LK

In this case we have considered our synthetic sequences, as well as, the Middlebury database and we have compared to evaluation of the integrand.

In figure 3 we plot the confidence measures κ and E_{LKV} versus the end-point-error EE for variational LK (with no warping) for the same representative synthetic sequences shown in the previous section. Although, the smoothness term of the variational distorts the decreasing pattern of fig. 2, we still have a clear decreasing dependency between κ and EE. However, this is not the case between E_{LKV} and EE, which plots do not present a defined dependency (neither increasing nor decreasing).

In figure 4 we plot the confidence measures κ and E_{LKV} versus the end-point-error EE for variational LK (with warping) considering the representative sequences of the Middlebury database. We have chosen a sequence with non-linear deformation (Dimetrodon in first columns), a sequence with textured objects and linear motion (Grove2 in second columns) and a sequence with non-textured objects and linear motion (Urban3 in third columns). Equivalent to the synthetic sequences, we have a decreasing dependency between κ and EE. We expect an increasing dependency between E_{LKV} and EE, thus, the plots should draw a parabola. That is, we expect low values of EE for values of E_{LKV} close to 0, and high values of EE for values of E_{LKV} close to 1. In this case we do not observe a clear increasing dependency.

Tables 2 and 3 show Spearman coefficient ρ and the $p-$value for the unilateral tests $TP1$ and $TP2$ considering the synthetic and the Middlebury databases respectively. As expected, the Spearman correlation coefficient achieves negative values for κ versus EE and the $p-$value is of the order of 10^{-16}, so that, there is a negative dependency between κ and EE. However, ρ does not achieve high positive values for E_{LKV} versus EE, which is reflected in $p-$values close to 1.

	κ		E_{LKV}	
	ρ	$p-$val	ρ	$p-$val
Dimetrodon	-0.53	0.00	-0.62	1.00
Grove2	-0.62	0.00	-0.46	1.00
Grove3	-0.57	0.00	-0.41	1.00
Hydrangea	-0.69	0.00	-0.62	1.00
RubberWhale	-0.56	0.00	-0.26	1.00
Urban2	-0.63	0.00	-0.69	1.00
Urban3	-0.58	0.00	-0.58	1.00
Venus	-0.60	0.00	-0.58	1.00

Table 3: Spearman tests $TP1$ (for κ) and $TP2$ (for E_{LKV}) for variational LK considering the Middlebury database.

5.3. Application to autonomous navigation

In this section we show that the confidence measure can also be used to assess autonomous navigation.

Figure 5 shows the condition number and the computed optical flow for the Endepa sequences: ConstructionSite, CrazyTurn and InternOnBike. The OF is expected to be convergent to a vanishing point, and cars and objects having a different motion. Notice that for these sequences we have a reflectance over the bonnet and in that region, the flow of the above part is reflected.

In figure 5, first row images show a representative frame of the Endepa sequences with regions having a good confidence measure enclosed by black lines and filled in red. For those regions with a good confidence measure we expect a reliable OF computation, while, for regions with low values of κ we expect a random computation of the OF. Second row images show the OF associated to the confidence measure shown on above images. Notice that for regions with good κ, OF is always as expected, while regions with low κ, OF direction is random. In fig. 5(d) there is an example where the OF is accurate for low values of κ whereas in the other two images (figs. 5(e) and (f)), the OF is deviated for low values of κ. Therefore, κ can assess in which regions of the sequence OF is properly computed.

6. Summary and Future Work

In spite of the advances in the design of variational schemes, confidence measures are rarely addressed in the

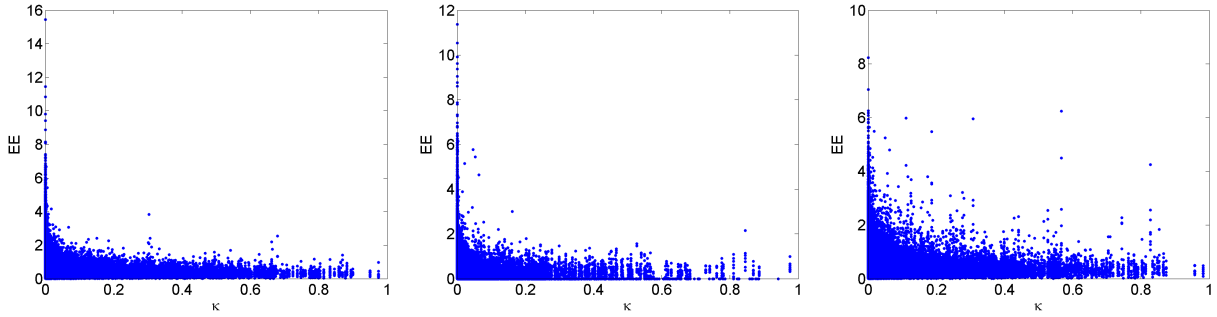

(a) Seq1 H (b) Seq2 M (c) Seq3 D

Figure 2: Point cloud plots for local LK for three representative synthetic sequences. κ versus EE.

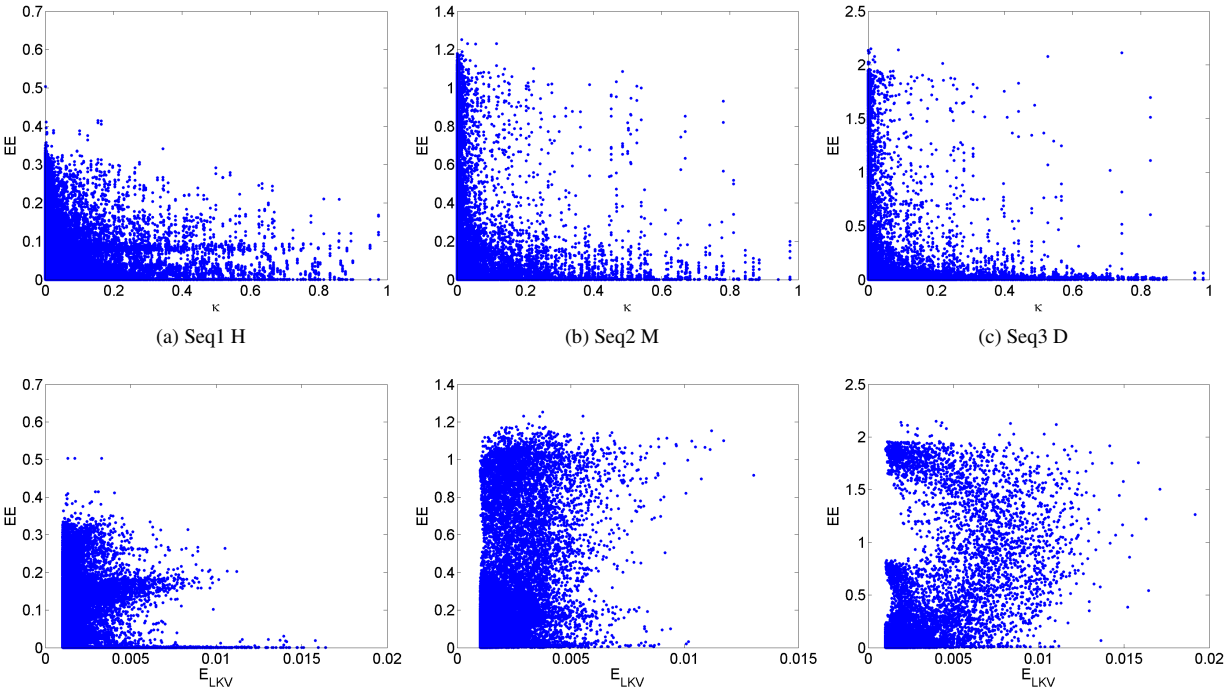

(a) Seq1 H (b) Seq2 M (c) Seq3 D

(d) Seq1 H (e) Seq2 M (f) Seq3 D

Figure 3: Point clouds plots for variational LK for three representative synthetic sequences. κ versus EE in first row and E_{LKV} versus EE in the second one.

literature. However, for their reliable application to navigation systems, we need a confidence measure to determine in which points the estimation is accurate. This paper reports an error analysis for Lukas-Kanade approaches and introduces a local confidence measure for global (variational) and local approaches. We compare our measure to an existing quantity in terms of their correlation to end-point-errors.

For sequences with ground truth (self-made synthetic sequences and the Middlebury database), our confidence measure presents a good correlation with flow errors for a local and a global approach. We found out that the existing quantity failed to present the expected correlation. Experiments on sequences for driving assistance show that a drop in our confidence measure implies that an erratic random direction of the computed optical flow, while high values ensure stable and coherent flows.

There are some improvements that should be done in the near future. First we note that for variational approaches, A_{LK} should be replaced by the matrix associated to the discretization of the Euler-Lagrange system. Second, in order

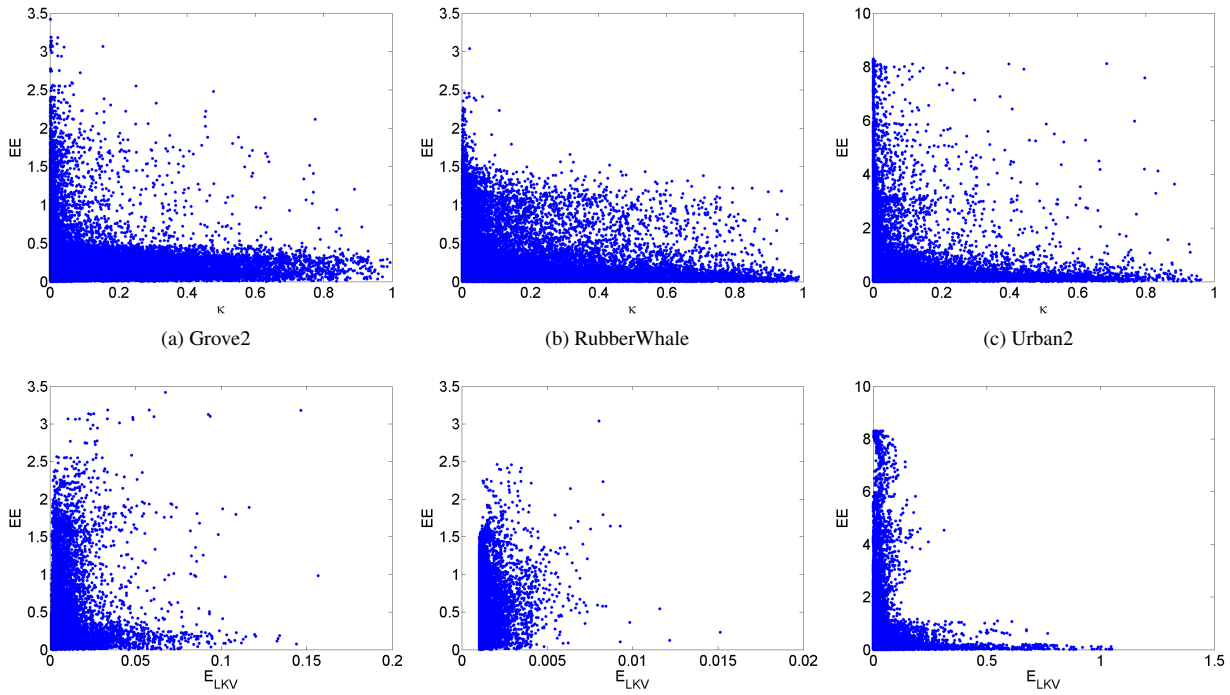

(a) Grove2 (b) RubberWhale (c) Urban2

(d) Grove2 (e) RubberWhale (f) Urban2

Figure 4: Point clouds plots for variational LK for the Middlebury sequences: Grove2, RubberWhale and Urban2. κ versus EE in first row and E_{LKV} versus EE in the second one.

	H				M				D			
	κ		E_{LKV}		κ		E_{LKV}		κ		E_{LKV}	
	ρ	$p-$val	ρ	$p-$val	ρ	$p-$val	ρ	$p-$val	ρ	$p-$val	ρ	$p-$val
Seq1	-0.59	0.00	-0.38	1.00	-0.61	0.00	0.02	0.23	-0.59	0.00	0.05	0.09
Seq2	-0.57	0.00	-0.29	1.00	-0.58	0.00	-0.06	0.98	-0.59	0.00	-0.11	1.00
Seq3	-0.62	0.00	-0.43	1.00	-0.58	0.00	-0.08	1.00	-0.58	0.00	-0.07	1.00

Table 2: Spearman tests $TP1$ (for κ) and $TP2$ (for E_{LKV}) for variational LK considering the Synthetic database.

to ensure a practical application, we should statistically determine which is the minimum value of the confidence measure ensuring a given predefined accuracy. Finally, it would be interesting to compare our confidence measure to other ones.

Acknowledgements. This work was supported by the Spanish projects PI071188, TIN2009-13618, TRA2010-21371-C03-01, CSD2007-00018 and the 2nd author by The Ramon y Cajal Program.

References

[1] Endepa project. http://www.mi.auckland.ac.nz/.

[2] Middlebury database. http://vision.middlebury.edu/flow/.

[3] Variational Lucas-Kanade implementation. http://people.csail.mit.edu/celiu/OpticalFlow/.

[4] S. Baker, D. Scharstein, J. Lewis, S. Roth, M. J. Black, and R. Szeliski. A database and evaluation methodology for optical flow. *IJCV*, 92(1):1–31, 2011.

[5] J. L. Barron, D. J. Fleet, and S. S. Beauchemin. Performance of optical flow techniques. *IJCV*, 12(1):43–77, 1994.

[6] J. Bigün, G. H. Granlund, and J. Wiklund. Multidimensional orientation estimation with applications to texture analysis and optical flow. *PAMI*, 13(8):775–790, 1991.

[7] J. Bouguet. Pyramidal implementation of the Lucas Kanade feature tracker description of the algorithm, 2000.

[8] A. Bruhn, J. Weickert, and C. Schnörr. Lucas/Kanade meets Horn/Schunck: Combining local and global optic flow methods. *IJCV*, 61(2):221–231, 2005.

[9] W. Cheney and D. Kincaid. *Numerical Mathematic and Computing, Sixth edition*. Bob Pirtle, USA, 2008. ISBN-13:978-0-495-11475-8.

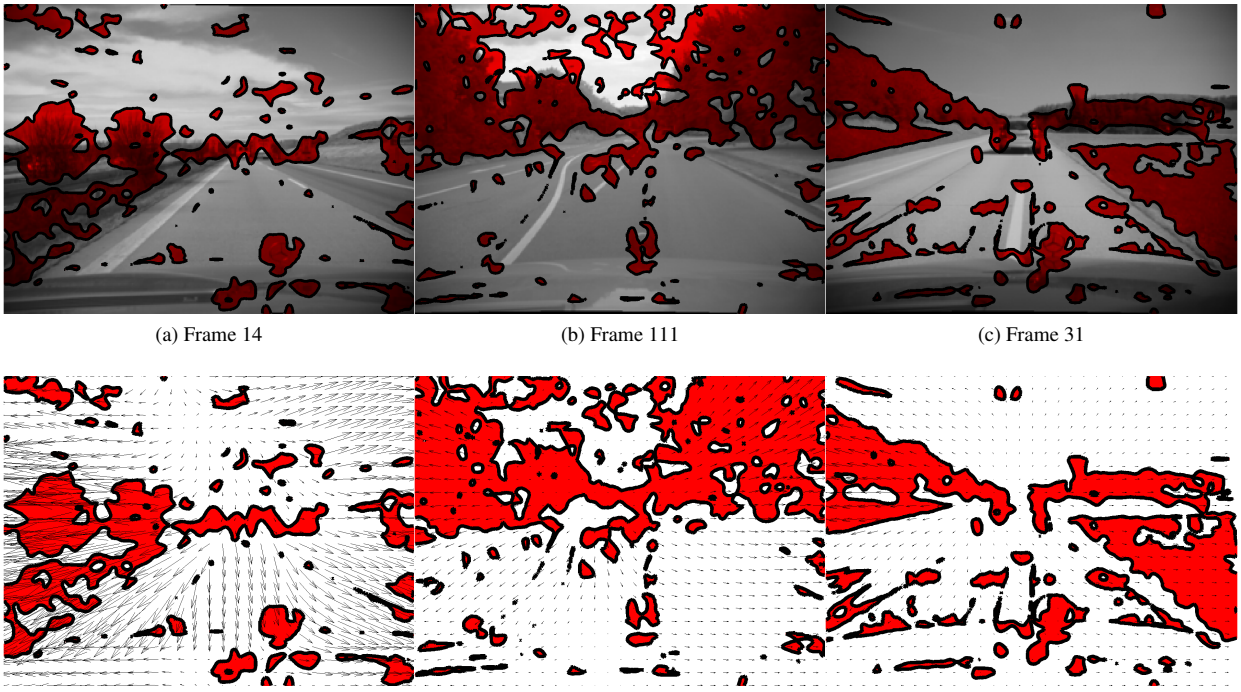

(a) Frame 14 (b) Frame 111 (c) Frame 31

(d) OF frame 14 (e) OF frame 111 (f) OF frame 31

Figure 5: In rows, the ConstructionSite, the CrazyTurn and the InternOnBike sequences respectively. First column shows a representative frame with regions having high values of κ enclosed by red lines. Second and third columns show the computed OF between the indicated frame and the next one. The OF is shown as motion vectors over the flow color scheme.

[10] J. García-Barnés. Variational framework for assessment of the left ventricle motion. *Mathematical Modelling of Natural Phenomena*, 3(6):76, 2008.

[11] B. Horn and B. Schunck. Determining optical flow. *Artificial Intelligence*, 17:185–203, 1981.

[12] B. Jähne. *Spatio-Temporal Image Processing. Lecture Notes in Computer Science*, volume 751. Springer Berlin / Heidelberg, Berlin, 1993. ISSN:0302-9743.

[13] C. Liu. *Beyond pixels: exploring new representations and applications for motion analysis*. PhD thesis, Cambridge, MA, USA, 2009.

[14] B. Lucas and T. Kanade. An iterative image registration technique with an application to stereo vision. In *DARPA IU Workshop*, pages 121–130, 1981.

[15] J. L. Myers and A. D. Well. *Research Design and Statistical Analysis 2Ed.* Lawrence Erlbaum Associates, New Jersey, 2009. ISBN:0-8058-4037-0.

[16] H. H. Nagel and W. Enkelmann. An investigation of smoothness constraints for the estimation of displacement vector fields from image sequences. *PAMI*, 8:565–593, 1986.

[17] S. Roth and M. Black. On the spatial statistics of optical flow. *IJCV*, 74(1):33–50, 2007.

[18] J. Sánchez and R. K. E. Destefanis. Estimating 3d flow for driver assistance applications. In *3rd Pacific Rim Symposium on Advances in Image and Video Technology*, pages 237–248, 2008.

[19] A. Singh. An estimation-theoretic framework for discontinuous flow fields. In *ICCV*, pages 168–177, 1990.

[20] D. Sun, S. Roth, and M. J. Black. Secrets of optical flow estimation and their principles. In *CVPR*, pages 2432–2439, 2010.

[21] S. Uras, F. Girosi, A. Verri, and V. Torre. A computational approach to motion perception. *Biol. Cybern.*, 60:79–97, 1988.

[22] A. M. Waxman, J. Wu, and F. Bergholm. Convected activation profiles and the measurement of visual motion. *Proc. IEEE CVPR*, pages 717–723, 1988.

[23] M. Werlberger, T. Pock, and H. Bischof. Motion estimation with non-local total variation regularization. In *CVPR*, pages 2464–2471, 2010.

[24] C. Yu, H. Ju, and Y. Gao. 3d virtual reality simulator for planetary rover operation and testing. In *2009 IEEE international conference on Virtual Environments, Human-Computer Interfaces and Measurement Systems*, pages 101–106, 2009.

[25] C. Zach, T. Pock, and H. Bischof. A duality based approach for real-time TV-L1 optical flow. *Pattern Recognition (Proc. DAGM)*, pages 214–223, 2007.

[26] H. Zimmer, A. Bruhn, and J. Weickert. Optical flow in harmony. *IJCV*, 93:368–388, 2011.